Calculations of Flow Resistance in the Juxtacanalicular Meshwork

C. Ross Ethier,* Roger D. Kamm,* Bryan A. Palaszewski,* Mark C. Johnson,*† and Thomas M. Richardson†

The structure of the juxtacanalicular meshwork (JCM) was analyzed morphometrically, and the resulting data were used to calculate the resistance to flow through this tissue. Two models of the JCM were presented and compared. In the first (Model A), aqueous humor was assumed to flow via open channels within a solid framework, while, in the second (Model B), these open spaces were assumed to be filled with extracellular matrix gel. An expression giving the resistance of such a gel as a function of gel concentration was presented and tested on corneal and scleral stroma. Morphometry of normal and glaucomatous human eyes showed that Model A underpredicted the resistance of the JCM by factors of 10–100, suggesting that a GAG or proteoglycan gel may control the flow resistance of this tissue. This was supported by Model B, which showed that measured bulk concentrations of GAGs were consistent with gel concentrations needed to account for the estimated resistance of the JCM in vivo. Some limitations and implications of Model B were discussed. Invest Ophthalmol Vis Sci 27:1741–1750, 1986

There have been numerous attempts to identify the primary site of resistance in the aqueous outflow system. McEwen's[1] calculations of flow resistance based on the dimensions of the flow passages in the inner aspects of the meshwork indicated that both the uveal and corneoscleral meshwork should have negligible flow resistance, consistent with Grant's finding[2] that removal of the uveal meshwork had little effect on facility. Grant[3] later demonstrated that 75% of the resistance resided between the anterior chamber and the aqueous veins, suggesting that the dominant site of resistance was located proximal to the aqueous veins. This conclusion has been supported by estimates of the resistance associated with the aqueous veins and collector channels[4] and studies of the flow resistance of Schlemm's canal,[5,6] although recent work suggests that, at normal pressures, the collector channels may be more resistive than previously believed.[7] Based on these findings, many researchers have studied the corneoscleral and/or juxtacanalicular meshwork (JCM), in an attempt to identify the underlying cause of outflow resistance.

In this paper we focus upon the JCM, and, in particular, analyze its structure and thus compute the resistance to flow through this tissue. This requires detailed and quantitative information concerning the local morphology and a computational model capable of predicting flow resistance based on the salient morphological features. Some of the necessary morphometric data on the JCM have already appeared in the literature,[8,9] such as area of the extracellular regions, area of the optically clear spaces, and cell area. These variables are needed input for the computational model used in this study, in which the JCM is treated as a porous material.

Recent studies have also provided data on the biochemical composition of the trabecular meshwork. Knepper et al[10,11] have determined the gross amounts of glycosaminoglycans (GAGs) in excised trabecular meshwork, while Richardson[12] has used ruthenium red staining to determine the distribution of GAGs within the JCM. These data are useful in predicting what effect proteoglycan gels within the JCM extracellular spaces may have on the flow resistance of this porous tissue.

This paper describes two computational models that predict the flow resistance of the juxtacanalicular meshwork. In the first model (Model A), we describe the JCM as a porous medium permeated by open spaces (pores) through which the aqueous humor flows. In the second model (Model B), we allow the open spaces of the JCM to be filled with a GAG gel, and predict the flow resistance of this gel and, hence, of the

From the *Department of Mechanical Engineering, Massachusetts Institute of Technology, Cambridge, Massachusetts, and the †Howe Laboratory of Ophthalmology, Massachusetts Eye and Ear Infirmary, Harvard Medical School, Boston, Massachusetts.

Supported by NIH Grants EY05503, EY03141, and EY02655, and a Whitaker Health Sciences Fund Grant. CRE acknowledges financial support from the Alberta Heritage Foundation and the Natural Sciences and Engineering Research Council of Canada.

Submitted for publication: August 14, 1985.

Reprint requests: Professor Roger D. Kamm, Department of Mechanical Engineering, Massachusetts Institute of Technology, Cambridge, MA 02139.

JCM as a whole. Before describing the specific models, a brief overview of porous media theory as applied to the JCM is presented.

The JCM as a Porous Material

Porous Media Theory

The theory of flow through porous media has been used to successfully predict the flow resistance of various porous materials, ranging from geological structures to human cartilage. In the eye, similar methods have been employed to study the permeability of the cornea by Bert and Fatt[13] and Hedbys and Mishima.[14]

A porous material is broadly defined as any substance comprised of a solid framework, through which fluid can pass. Typically, the flow is described by porous media theory whenever it would be too difficult or cumbersome to treat each fluid passageway individually. The simplest porous structures consist of a collection of circular, cylindrical pores in an otherwise solid block. The resistance to flow through a single pore in this block would be given by the ratio of pressure drop to flow rate ($\Delta P/Q$), and could be calculated, in this instance, using the relationship for Poiseuille flow:

$$R = \frac{\Delta P}{Q} = \frac{8\mu L}{\pi a^4}, \quad (1)$$

where μ is the fluid viscosity, a is the pore radius, R is the block's resistance, and L its length. For a block containing N identical pores connecting the high and low pressure sides, the total flow rate would be increased N-fold, and the total resistance would therefore fall to a value of

$$R = \frac{8\mu L}{N\pi a^4} \quad (2)$$

While the overall resistance is a useful result, it is often more convenient to describe a material in terms of its permeability. Permeability is a local material property that is independent of the gross dimensions of the porous material or the properties of the permeating fluid, but depends, instead, on the characteristics of the pores themselves.

Permeability (**K**) is related to resistance by the expression (Darcy's law):

$$R = \frac{\mu L}{KA}, \quad (3)$$

where A is the total cross-sectional area across which the flow takes place.

In the example given above (equation 2), the permeability is simply $n\pi a^4/8$, where $n = N/A$ is the number of pores per unit area. Since permeability is a local property, it can be calculated from simple measurements made, for example, from any small fragment of the material, provided that the fragment contains a sufficient number of pores so as to be representative of the whole.

Most porous materials, however, have a more complex geometry than that of our simple example. Kozeny and Carman[15] developed a general expression for permeability, which has been used successfully in porous materials of widely differing geometries. They related the permeability to two geometrical parameters: the porosity, ϵ (the ratio of void volume to total volume), and the specific surface, S (the ratio of wetted pore surface area to total volume). The expression they obtained is

$$K = \frac{\epsilon^3}{k * S^2}, \quad (4)$$

where k is known as the Kozeny constant and depends only on the pore geometry (e.g., $k = 2$ for straight circular cylindrical pores). The Kozeny constant as it appears in equation 4 incorporates pore tortuosity effects, and for a typical low porosity porous material with tortuous (rather than straight) pores, will lie in the range of three to five.

The Carman-Kozeny equation (equation 4) thus provides a well-established indirect method for estimating the permeability of a material via measurement of the porosity and specific surface. While many different methods have been reported for determining these parameters, in analyzing the JCM, we have simply measured porosity and specific surface directly from transmission electron micrographs of this tissue. To verify that photomicrographs can indeed be used in this manner, we used this technique to determine the permeability of various open-pore foams.[16] The permeabilities predicted from these photomicrographs agreed well with measured permeability values.

Specific Features of the JCM

A necessary step in the development of a porous media model of the JCM is the characterization of this tissue's flow passages. We assume that, for all practical purposes, the trabecular meshwork cells are impermeable, and, therefore, focus our attention on the ultrastructural composition of the extracellular space as seen in transmission electron micrographs. This space contains a variety of components which have been grouped in various ways in the past.

For modelling purposes, we have found it convenient to divide the extracellular space into three broad subdivisions: "solids," gray amorphous material, and open spaces. The first category ("solids") includes all electron-dense extracellular material; namely, elastin fibers, collagen fibers, and amorphous fibrillar material (Type C material of Lütjen-Drecoll[8]). Due to their density and structure, we assume these substances to be im-

permeable. The second category is made up of the gray amorphous material (fine fibrillar material, ground substance, type A material of Lütjen-Drecoll[8]) which usually abutts against the "solids" described above. A substantial body of evidence, for example, that presented by Richardson[12] and Armaly and Wang,[17] indicates that this amorphous material is, to a large degree, composed of GAGs and glycoconjugates. Its optical density is variable, and, in some extracellular locations, this material appears to be absent altogether. Finally, the third category, referred to as "open spaces" or pores, includes all regions which contain neither amorphous material nor solids. These open spaces may be fixation artifacts, in that, in vivo, they also may have been filled with gray amorphous material.[18]

Characterization of Extracellular Matrix Permeability

For the purposes of Model B, the flow resistance of the gray amorphous material must be estimated. It is presumed that its resistance is primarily due to a GAG or glycoconjugate gel, so that our problem is reduced to one of estimating the hydrodynamic resistance of such a gel. For our present purposes, a gel can be envisioned as a crosslinked (or entangled) array of randomly oriented polymers. A common idealization involves modelling the gel-forming polymers as cylindrical fibers (the fiber matrix model) (e.g., Ogston et al[19]). This same idealization was employed by Curry and Michel[20] to successfully describe the permeability characteristics of the frog mesenteric capillary wall.

A viscous flow analysis is used to predict the flow resistance of this fiber matrix, and an expression is obtained which relates the gel permeability to its concentration and the fiber (gel-forming polymer strand) radius.[21]* By fitting this result to experimental data so as to determine the fiber radius, a semi-empirical expression is obtained which relates gel permeability ($\mathbf{K}_0$) to gel concentration. In order to simplify the calculations, the mathematical expression derived from the fiber matrix model can be fit by the approximate relationship

$$\mathbf{K}_0 = 0.319\, a_0^2 (c * \bar{v})^{-1.17}, \qquad (5)$$

where c is the gel concentration (g/ml), $\bar{v}$ is the specific volume of the gel-forming material (ml/g), and a_0 is the fiber (polymer) radius. (Note that the product $c*\bar{v}$ is the gel solid fraction.) This relationship is accurate within 5% for values of $c*\bar{v}$ between 6.0×10^{-5} and 1.3×10^{-2}, which corresponds well to many physiological situations.

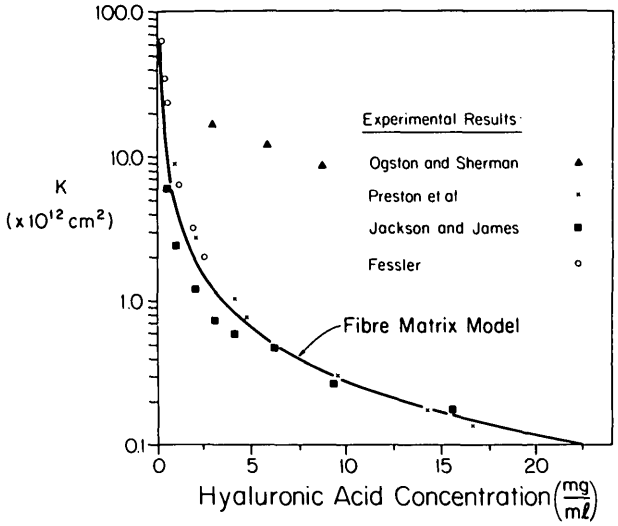

Fig. 1. Graph of hyaluronic acid permeability (K) vs hyaluronic acid concentration, showing a comparison between experimental data and the results of the fiber matrix model (for a fiber radius of a = 5Å). Data from Preston et al[22] and Fessler[23] are derived from sedimentation studies (see Fessler and Ogston,[24] Ethier[25]). It is not known why the results of Ogston and Sherman[26] differ from those of other investigators.

For the particular case of hyaluronic acid, a fiber radius of 5 Å produces close agreement between the theoretical prediction and experimental measurements (Fig. 1).[21] In the absence of contrary information, a 5 Å radius is assumed to be appropriate for all GAG gels.

Accepting the approximate validity of this approach, equation 5 can be used to calculate the local gel permeability in the extracellular spaces, $\mathbf{K}_0$. The net permeability of a given tissue (e.g., the JCM) is then obtained by noting that the "impermeable" components of the tissue simply act to decrease the available area for fluid flow. If the bulk porosity e is defined as:

$$e = 1 - \frac{\text{volume of impermeable components}}{\text{total volume}},$$

the net permeability of the tissue is given by

$$\mathbf{K} = e\mathbf{K}_0, \qquad (6)$$

and equation (3) can be used to obtain the resistance of the entire tissue.

Assumptions and Methods

Model A

Model A assumes that the "open spaces" within the JCM are present in vivo (i.e., are not artifactual). Thus,

* Since all porous media theories are based on the assumption that the fluid can be treated as a continuum (i.e., as a homogeneous substance with properties such as viscosity defined on a scale much smaller than any physical dimension of the system), the validity of this approach might be questioned. However the derivation of the Stokes-Einstein diffusion coefficient produces accurate results from similar assumptions. Furthermore, the excellent agreement with experiment (Fig. 1) suggests that this approach is valid.

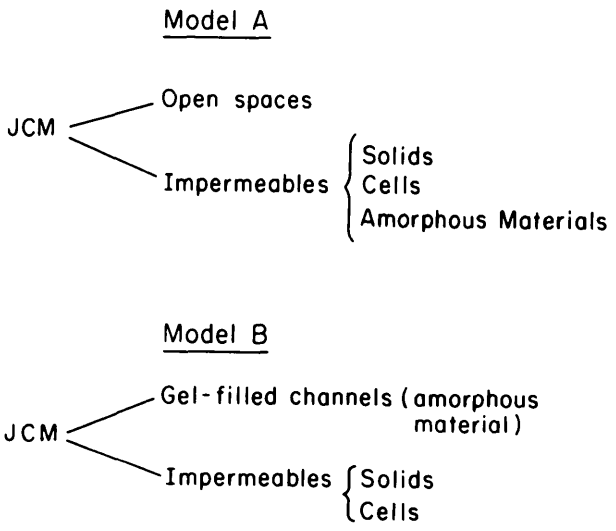

Fig. 2. Assumptions regarding JCM structure made in developing Models A and B. No fluid is assumed to pass through "impermeables." "Solids" are made up of collagen, elastin and fibrillar material. Fluid passes through open spaces in Model A and gel-filled channels in Model B.

fluid passes only through these open spaces, and is excluded from the amorphous material and solids (i.e., from the entire extracellular matrix). This approach is based on the knowledge that the resistance to flow through the amorphous material is much greater than through unobstructed pores, as well as a desire to maximize the predicted flow resistance of this tissue. Model A, therefore, considers the amorphous material to be impermeable, and treats the JCM as a two-component system: open spaces and impermeables ("solids," cells, and amorphous material) (Fig. 2).

To determine the resistance to flow through these open spaces, the JCM porosity and specific surface were therefore measured from photomicrographs. We examined human specimens obtained from the New England Eye Bank (controls) and excised during filtering surgery (glaucomatous). Specimens were fixed overnight by immersion in 3% glutaraldehyde in 0.1 M cacodylate buffer, pH = 7.3. After being rinsed three times in 0.1 M cacodylate buffer, the samples were postfixed for 2 hr at room temperature in 1% osmium tetroxide in 0.2 M cacodylate buffer. Specimens were prepared for transmission electron microscopy by dehydration in ethyl alcohol, embedding in Epon 812, and sectioning. Thin sections were stained with uranyl acetate and lead citrate. Micrographs had final magnifications between 6200× and 7000×. Fixation at conditions of zero pressure should tend to minimize the amount of open space,[27] and thereby produce estimates of flow resistance somewhat larger than normal.

A region extending 7–10 μm interiorly from the inner wall of Schlemm's canal was analysed in each micrograph using an Apple II computer and a digitizing pad. Each apparently "open" space was traced with a stylus, from which the computer determined both the open area and the perimeter. Open spaces were defined by a decided lack of cellular, fibrillar, or amorphous material. In the analysis of micrographs, porosity and specific surface are taken as void area divided by total area and wetted pore perimeter divided by total area, respectively. A typical micrograph is shown in Figure 3, with the selected "open spaces" highlighted.

The effect of non-uniformity within the JCM was modelled by dividing the analysed region into 40 subdivisions (2.5 μm by 5 μm) and computing an individual specific surface and porosity for each sub-region. The size of each subdivision was selected so that the distance over which significant variations in pore size or pore density were observed was greater than the dimensions of the subdivision. These data were then used in equation 4 to produce a distribution containing 40 values of permeability for each micrograph analyzed. The entire meshwork was then modelled by assuming it to consist of a large number of rectangular blocks $2.5 \times 5 \times 5$ μm in size. The permeability of each block was randomly selected from the distribution obtained by the 40 sub-region measurements, with the assumption that the sub-regions analyzed were representative of the entire JCM. The resulting network was then numerically analysed to determine its overall flow resistance.

In addition to resistance values obtained via this numerical technique, JCM resistance was calculated from equations 3 and 4 using bulk (JCM average) values for specific surface and porosity. The Kozeny constant k was assigned a value of four, as is appropriate for a random, tortuous porous material.[15] In all calculations, the viscosity of aqueous humor at 37°C was taken as 0.72 centipoise,[5] while the flow-normal area of the JCM was taken to be 0.11 cm^2 (36 mm in circumference with a meridional width of 300 μm[5]). Resistances were calculated for flow-wise lengths of the JCM of 10 and 25 μm. This procedure was followed in micrographs from four eyes: two control eyes, one pigmentary glaucomatous eye, and one primary open angle glaucomatous (POAG) eye. In total, five micrographs were studied: two micrographs from one control eye, and one micrograph each from the second control eye, the POAG eye, and the pigmentary glaucomatous eye. The area of the analyzed region within each of the above micrographs was 230, 175, 267, 234, and 205 μm^2, respectively.

Model B

In Model B, the JCM is viewed as an impermeable matrix of cells and "solids" (collagen, elastin, fibrillar material), within which is distributed a network of flow channels completely filled with a homogeneous GAG

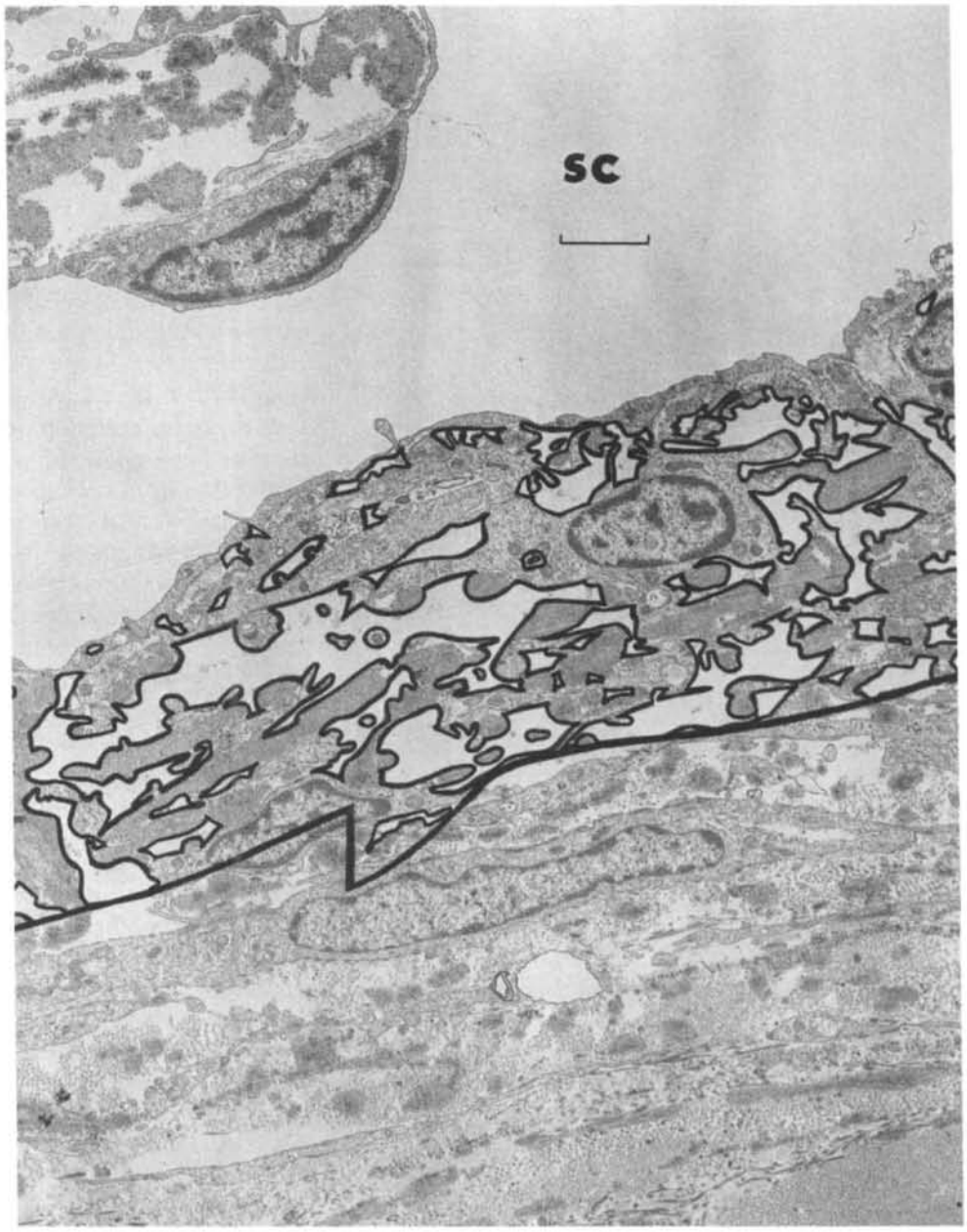

Fig. 3. Region from the JCM of a control eye, with open spaces highlighted. The analyzed region extends interiorly from the inner wall of Schlemm's canal to the heavy line. SC: lumen of Schlemm's canal, calibration bar: 2.5 μm.

or proteoglycan gel (Fig. 2). We note that the resistance of a GAG-filled meshwork would be sensitive to exogenous hyaluronidase perfusion, and, although this sensitivity has been shown in sub-primates, the data on primates is conflicting (e.g., Knepper et al[11]).

Denoting the global porosity as used in Models A and B by e_A and e_B, respectively, we see that, since the amorphous material is no longer considered impermeable:

$$e_B = e_A + \frac{\text{area of amorphous material}}{\text{total area}}$$

Due to the uncertainty in the values of e_A and the relative amount of amorphous material, we simply present results for an appropriate wide range of porosities e_B.

Ideally, the model requires quantitative knowledge about GAG and glycoconjugate distributions in the extracellular void spaces. Qualitatively, it has been felt that an appreciable fraction of the total meshwork GAG population is found in the voids, as suggested by the strong ruthenium red[12] and alcian blue[28] staining of these spaces. Unfortunately, a more quantitative description is presently unavailable, and, therefore, we adopt the approach of predicting the void space GAG concentration necessary to account for the estimated pressure drop across the JCM.

Thus, we suppose that the JCM is the major site of resistance to flow, and from equations 3, 5, and 6 cal-

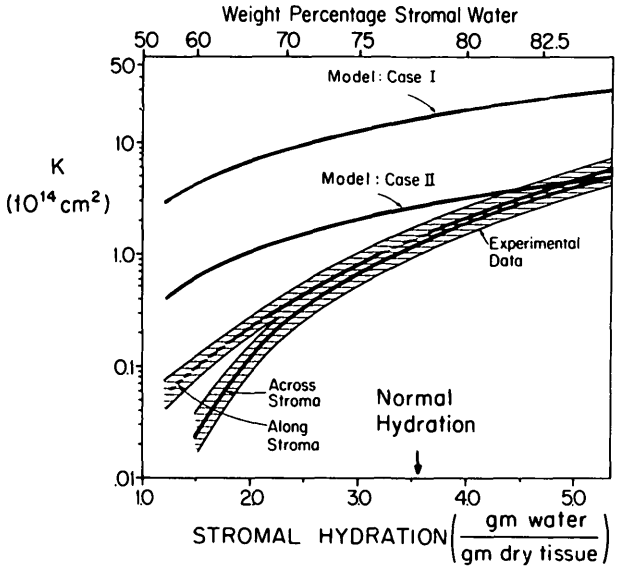

Fig. 4. Graph of bovine corneal stromal permeability (K) versus stromal hydration, showing a comparison between the experimental data of Hedbys and Mishima[14] and theoretical predictions. Case I: GAG-generated resistance only; Case II: proteoglycan-generated resistance. The shaded region indicates the range of uncertainty in the experimental data.

culate the concentration of a pure GAG gel within the empty spaces of the JCM required to produce a given pressure drop. Values for flow-normal area (A) and viscosity (μ) are as reported for Model A, and a specific volume of $\bar{v}$ = 0.67 ml/g was used for GAGs.[22]

Results

Fiber Matrix Model

In order to test the validity of the fiber matrix model in a physiological context, we studied the permeability of corneal and scleral stroma. These tissues were selected as they are well-characterized extracellular tissues whose flow resistance is due mainly to GAGs or proteoglycans.[14,29] Concentrations of the extracellular components within corneal and scleral stroma were obtained from the literature to produce a typical concentration profile for bovine corneal stroma and rabbit scleral stroma.[25] These profiles allowed us to estimate the concentration of GAGs or proteoglycans in the void spaces (i.e., the extracellular water-filled spaces) of each tissue for various stromal hydrations. Equations 5 and 6 were then used to calculate stromal permeability as a function of stromal hydration. Two scenarios were considered: in the first, only GAGs contributed to flow resistance, while, in the second, the entire extracellular proteoglycan complex (GAG plus associated protein) influenced flow resistance.†

† Details of permeability calculations for a two-component fibrous medium (GAGs plus proteins) are set forth in reference 25.

The results of these calculations for corneal stroma are compared with the experimental data of Hedbys and Mishima[14] in Figure 4.‡ The permeability predicted in case II (proteoglycan-generated resistance) more closely matches the data than that predicted in case I, suggesting that the protein portion of the extracellular proteoglycan gel is an important determinant of flow resistance. At normal hydration, the agreement between theory (case II) and experiment is good (within a factor of two), although this agreement worsens at stromal hydrations much below normal. This discrepancy may result from a progressive alignment of proteoglycans in the plane of the stroma, as this tissue thins at lower hydration, while the model assumes a random distribution of fiber orientations. Introducing this effect into the model would more closely align theoretical predictions and experiment. A similar phenomenon may explain the difference in the experimental curves for flow along and across the stroma at low hydration, since in these two cases the proteoglycan fibers are, on average, oriented differently with respect to the flow, and thus have differing resistances. These effects become important only at unphysiologic (low) hydrations, and thus are not expected to influence predictions of the model.

An analysis of the permeability of the scleral stroma gives similar results; namely, that the entire extracellular proteoglycan complex is an important determinant of flow resistance. The measured permeability[29] of 1.3×10^{-14} cm^2 is approximately five times smaller than the value calculated via case II of 6.7×10^{-14} cm^2, representing slightly poorer agreement than that obtained for corneal stroma. This difference is, in part, due to greater uncertainties in the data on scleral composition, and, perhaps, to differences in proteoglycan composition between the cornea and the sclera. In summary, the fiber matrix model was felt to be sufficiently accurate for present purposes.

Model A

The percentage of open space within the JCM of normal eyes measured in this study is summarized in line 3 of Table 1, while lines 1 and 2 display previously reported values for the JCM. A large variation is apparent among the few reported figures for the JCM; the current study and that of Lütjen-Drecoll[8] present values greatly different from those of Lindenmayer et al.[9] This probably reflects the fact that only the latter study utilized samples fixed at pressure.

‡ The bovine corneal composition used was: collagen 18.0% (14.0%), water 78% (83.4%), salts 0.9% (0.27%), GAGs 0.95% (0.69%), GAG-associated protein 1.55% (1.13%), and free protein 0.6% (0.47%).[25] Values are weight (volume) percentages.

Table 2 displays measured values for gross JCM porosity and specific surface for each of the micrographs analyzed. Interestingly, the results of the permeability calculations based on gross JCM porosity and specific surface were nearly identical with those of the more sophisticated numerical model. This suggests that the use of JCM-average values for porosity (ϵ) and specific surface (S) in the Carman-Kozeny equation is acceptable, despite the apparent heterogeneity of the JCM. The computed resistances (based on gross JCM porosity and specific surface) are also given in Table 2, and compared to the estimated in vivo resistance of the JCM.

Significantly ($p < 0.005$, two-sided t-test), in normal eyes, the calculated resistance falls short of the estimated in vivo resistance by two orders of magnitude. In other words, the cells, collagen, elastin, and fibrillar material within the normal JCM are expected to account for no more than a few percent of this tissue's resistance. In addition, preliminary results (based on only one micrograph each), indicate that the calculated resistance of the JCM of POAG and pigmentary glaucomatous eyes falls short of the estimated in vivo resistance by factors of approximately 100 and 10, respectively. Due to its lower porosity, the pigmentary glaucomatous eye has a larger calculated resistance than the other eyes. Although no definite conclusions can be drawn regarding the glaucomatous eyes (due to the sample size of one), the results are highly suggestive.

Hence, in spite of efforts to overestimate JCM resistance, Model A is able to account for only a negligible fraction of the observed outflow resistance in normal eyes. We therefore considered several possible explanations for our failure to find even a significant fraction of the resistance: (1) What appear to be "open spaces" on the micrograph might well contain materials that are not visualized by routine electron microscopy (e.g., GAGs and other glycoconjugates), (2) the dimensions of the channels within the JCM have been substantially altered during tissue processing, or (3) the primary site of resistance resides elsewhere.

Of these, the first seemed most likely. Model B enables us to test this hypothesis.

Table 1. Quantitative morphology of normal primate trabecular meshwork

Reference	*% Optically Clear Space*†*	*Fixation Pressure*	*Species*
Lindenmayer et al[9]	59 ± 6.7%	15 mm Hg	Baboon, various monkey
Lütjen-Drecoll[8]	17 ± 7.7%	Zero (immersion)	Maccaca arctoides
Present study	23 ± 4.6%	Zero (immersion)	Human

* Mean ± standard deviation.

† Average porosity values measured within the JCM (either 7.5 or 10 μm wide region from Schlemm's Canal endothelium), as visualized by transmission electron microscopy.

Model B

Results of Model B for a JCM resistance of 2.5 mm Hg/μl/min (ΔP = 5 mm Hg, Q = 2 μl/min) are displayed in Figure 5, where the calculated gel concentration is plotted as a function of porosity, e_B. The range of results (Fig. 5, cross-hatched area) corresponds to JCM thicknesses between 10 and 25 μm. The predicted gel concentrations in the void spaces of the JCM lie in the range 1.1–6.5 mg per ml void space.

It is useful to compare these predicted concentrations with GAG concentrations measured in normal (unperfused) whole rabbit aqueous outflow pathway tissue by Knepper et al.[10,11] Using reported hexuronic acid levels, one obtains an estimated GAG concentration in rabbit meshwork of approximately 1.0 mg GAG per ml solid tissue,§ which can be converted to a GAG concentration per unit volume of void space via

§ Reported values used in all calculations of meshwork GAG concentrations are: 7.5 nmole hexuronic acid/mg dry defatted tissue,[11] and a dry defatted meshwork weight of 0.72 mg.[10] In addition, the following assumptions were made: an average GAG molecular weight of 470 daltons/disaccharide unit, one hexuronic acid moiety per disaccharide unit, water plus fat content of 75% (by weight) for meshwork tissue, and a tissue density of 1.1 mg/ml.

Table 2. Comparison between calculated (via Model A) and estimated in vivo resistance*† of the JCM

		Porosity	*Specific Surface (μm^{-1})*	*Calculated Resistance‡ (mm Hg/μl/min)*	*Estimated Resistance (mm Hg/μl/min)*
Normal eyes	Eye #1	0.246	1.29	0.035–0.089	2.5*
		0.264	1.31	0.029–0.074	
	Eye #2	0.177	0.79	0.035–0.088	
Pigmentary glaucomatous	Eye #3	0.069	0.77	0.56–1.41	15†
POAG	Eye #4	0.243	0.79	0.014–0.034	15†

* Based on assumed 5 mm Hg pressure drop across the JCM, and flowrate of 2 μl/min.

† Based on 30 mm Hg pressure drop and flowrate of 2 μl/min.

‡ Range corresponds to JCM thicknesses between 10 and 25 μm.

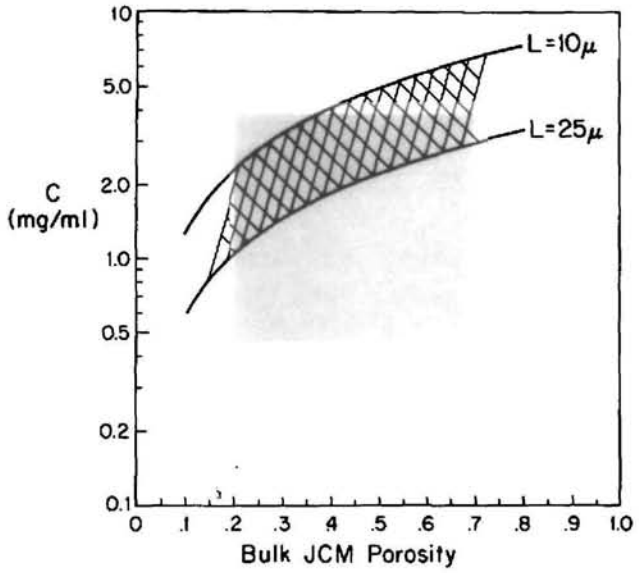

Fig. 5. Graph of void space gel concentration (c) required to produce a 5 mm Hg pressure drop across the JCM versus JCM bulk porosity, e_B. A flowrate of 2 μl/min was assumed. The cross-hatched region represents calculated results for JCM thicknesses between 10 and 25 μm. The horizontal extent of the shaded area represents the estimated range of JCM bulk porosities, while the vertical extent represents corresponding estimated GAG concentrations derived from the data of Knepper et al[10,11] by equation 7.

$$\frac{\text{mass GAG}}{\text{unit void volume}} = \frac{\text{mass GAG}}{\text{unit volume tissue}} \times \frac{\text{unit volume tissue}}{\text{unit total volume}} \times \frac{\text{unit total volume}}{\text{unit void volume}}$$

$$= (1.0\ \text{mg/ml}) \times \frac{1-e}{e} \qquad (7)$$

By using measured bulk GAG levels, equation 7 thus establishes a relationship between void space GAG concentration and porosity within the JCM. The range of GAG concentrations predicted in this manner (for porosities between 0.2 and 0.7) is indicated by the vertical extent of the shaded region of Figure 5. It can be see that the shaded region overlies the predicted GAG concentrations of Model B over most of the expected porosity range.

An alternate method of estimating void space GAG concentrations is to divide the total estimated meshwork GAG mass (2.5×10^{-3} mg) by the total meshwork volume, calculated as 1.1×10^{-3} cm^3 (based on the reported cross-sectional area of 100 μm by 350 μm,[10] and assuming a circumferential length of 3.1 cm). This ratio, representing GAG mass per total meshwork volume, can be divided by meshwork bulk porosity to estimate void space GAG concentration. One possible error inherent in this method is that the excised tissue dimensions reported by Knepper et al[10] may not be representative of in situ dimensions. This discrepancy may be due to alterations in meshwork tissue volume which occurred during the dissection process. In fact, using these meshwork dimensions and the reported dry defatted meshwork weight produces a tissue density of over 2 g/cm^3 (based on water plus fat content of 75%), which is unreasonably high. Nevertheless, using this method to recalculate the bounds for the shaded area of Figure 5 indicates that void space GAG concentrations should lie between 3.3 and 11.5 mg/ml, somewhat higher than those estimated via equation 7. The agreement with the predictions of Model B is once again satisfactory, given the approximate nature of the GAG estimates from experimental data. However, in light of the concern over in situ meshwork dimensions, we are more confident of our concentrations estimated via equation 7.

It is important to note that equation 7 implicitly assumes that all GAGs present in the aqueous outflow pathway reside within the extracellular void spaces, which is not strictly the case (e.g., Armaly and Wang[17]). Taking this into account would shift the shaded box in Figure 5 downward, the extent of the shift depending on the fraction of aqueous outflow pathway GAGs not found in the void spaces. Since this fraction is unknown, the shaded box in Figure 5 may be thought of as an upper bound on the actual void space GAG concentration.

Discussion

The results of this study point to an extracellular GAG or proteoglycan gel as being a significant determinant of outflow resistance. The evidence leading to this conclusion can be summarized as follows. Firstly, Model A clearly indicates that the JCM of normal eyes, as pictured in a transmission micrograph, is responsible for only a small fraction of the resistance to outflow. In other words, the cellular, collagenous, elastin, and fibrillar fractions of the normal JCM provide insignificant resistance to aqueous outflow. Recall also that, at every step in the calculation, an attempt was made to overestimate the actual resistance, thus lending additional support to this conclusion. Hence, from a fluid mechanical viewpoint, there must be additional structure, not visualized on transmission electron micrographs, which is largely responsible for aqueous outflow resistance. The presence of GAGs in the meshwork, their ability to form flow-resistive extracellular gels,[30] and the inability of transmission electron microscopy to visualize GAG gels on conventionally fixed samples[31] all point to a GAG or proteoglycan gel as the principal cause of outflow resistance. Furthermore, the results of Model B lend credence to this possibility, as they indicate that the required extracellular GAG concentrations are not inconsistent with measured con-

centrations. Thus, the presence of a resistive extracellular gel appears to be a viable possibility.

The results of Model A also suggest that the JCM of pigmentary and POAG eyes has a calculated resistance much lower than the estimated in vivo resistance. The analysis of further glaucomatous JCMs is needed, however, to confirm this result. (Interestingly, the calculated resistance of the pigmentary glaucomatous eye was higher than that of either the control or POAG eyes, although still insufficient to account for the estimated resistance.)

One unknown factor in Model A is the effect that tissue fixation and processing may have upon the samples. The fixation process is known to markedly increase aqueous outflow resistance,[32] suggesting that the resistance of the analyzed samples may have been higher than the estimated in vivo resistances of Table 2, and thus further strengthening the conclusions of Model A. On the other hand, the effects of post-fixational tissue processing on facility are unknown, as is the exact amount of tissue distortion and/or shrinkage due to fixation and processing. However, such changes would have to be substantial, given the severe underprediction of aqueous outflow resistance by Model A. In this sense, the results of Model A are quite robust.

It is also useful to point out the limitations of Model B. Firstly, the GAG concentrations derived from the measurements of Knepper et al (shaded region in Figure 5) are: (1) approximate, due to uncertainties regarding GAG distribution in the meshwork, and (2) based on data from sub-primates (rabbits). Further morphometric data on primate trabecular meshwork are needed to strengthen the conclusions of Model B. Specifically, knowledge of the meshwork porosity at physiological pressure and of GAG distribution within the meshwork is required. In the latter category, specific information regarding relative concentrations of intracellular, intrabeam, and void space GAGs is needed. Furthermore, as a gel located in both the JCM and outer aspects of the corneoscleral meshwork would be more resistive (due to the greater fluid path length) than a gel of the same concentration localized within the JCM, knowledge about the distribution of void space GAGs as a function of position between the anterior chamber and Schlemm's canal would be useful.

A final and critical unknown is the exact composition of the postulated gel within the meshwork void spaces. The results of calculations for corneal and scleral stroma indicate that the protein moieties of a proteoglycan gel can be responsible for considerable flow resistance. However, in the absence of contradictory information, the void space gels of Model B have been assumed to be pure GAG. Qualitatively, the effect of a proteoglycan (rather than a pure GAG) gel would be to decrease the GAG concentration required to produce a given pressure drop. This would correspond to a downward shift of the curves and cross-hatched region in Figure 5. Naturally, details of the void space gel composition will be a necessary datum for a more realistic version of Model B.

In short, the extent to which Model B reflects reality within the trabecular meshwork is largely limited by the scarcity of necessary input data. On the other hand, a potential fault, intrinsic to the model itself, is the assumption of local gel homogeneity within the void space. This assumption excludes the situation in which the void space gel is permeated by fluid flow channels. Proof of such structures (or other gel inhomogeneity) within the meshwork would necessitate a more sophisticated treatment than Model B.

It is interesting to note that a gel-filled meshwork would have a resistance which is relatively independent of compression in the flow-wise direction. This can be seen by combining equations 3, 5, and 6, and noting that, in one-dimensional compression, the extracellular void volume is proportional to the meshwork width L. The latter observation implies that the void space concentration would vary as 1/L, and that resistance R would vary as $L^{-0.17}$, i.e., would decrease very slowly with increasing L. This effect might well be masked in the normal eye by the strong dependence of Schlemm's canal resistance upon meshwork dimension.[6]

Key words: aqueous outflow resistance, juxtacanalicular meshwork, morphometry, extracellular matrix, modelling, gel, human eye

Acknowledgments

The authors wish to thank Peggy Sherwood and Matt Miller for technical assistance, and Dr. W. M. Grant for helpful suggestions.

References

1. McEwen WK: Application of Poiseuille's law to aqueous outflow. Arch Ophthalmol 60:290, 1958.
2. Grant WM: Facility of flow through the trabecular meshwork. Arch Ophthalmol 54:245, 1955.
3. Grant WM: Further studies on facility of flow through the trabecular meshwork. Arch Ophthalmol 60:523, 1958.
4. Tripathi RC: Pathologic anatomy of the outflow pathway of aqueous humor in chronic simple glaucoma. Exp Eye Res 25(Suppl):403, 1977.
5. Moses RA: Circumferential flow in Schlemm's canal. Am J Ophthalmol 88:585, 1979.
6. Johnson MC and Kamm RD: The role of Schlemm's canal in aqueous outflow from the human eye. Invest Ophthalmol Vis Sci 24:320, 1983.
7. Rosenquist RC, Epstein DL, Johnson M, Grant WM, and Melamed S: Resistance variation with perfusion pressure after trabeculotomy. ARVO Abstracts. Invest Ophthalmol Vis Sci 26(Suppl):159, 1985.
8. Lütjen-Drecoll E: Structural factors influencing outflow facility and its changeability under drugs. Invest Ophthalmol 12:280, 1973.
9. Lindenmayer JM, Kahn MG, Hertzmark E, and Epstein DL:

Morphology and function of the aqueous outflow system in monkey eyes perfused with sulfhydryl reagents. Invest Ophthalmol Vis Sci 24:710, 1983.
10. Knepper PA, Farbman AL, and Tesler AG: Aqueous outflow pathway glycosammoglycans. Exp Eye Res 32:265, 1981.
11. Knepper PA, Farbman AL, and Tesler AG: Exogenous hyaluronidases and degradation of hyaluronic acid in the rabbit eye. Invest Ophthalmol Vis Sci 25:286, 1984.
12. Richardson TM: Distribution of glycosaminoglycans in the aqueous outflow system of the cat. Invest Ophthalmol Vis Sci 22:319, 1982.
13. Bert JL and Fatt I: Relation of water transport to water content in swelling biological membranes. *In* Surface Chemistry of Biological Systems, Blank M, editor. New York, Plenum Press, 1970, pp. 287–294.
14. Hedbys BO and Mishima S: Flow of water in the corneal stroma. Exp Eye Res 1:262, 1962.
15. Carman PC: Flow of Gases Through Porous Media. London, Butterworths Scientific Publications, 1956.
16. Donnelly EM: Permeability Measurements of Compressible Porous Media. SM Thesis, Department of Mechanical Eng., M.I.T., 1982.
17. Armaly MF and Wang Y: Demonstration of acid mucopolysaccharides in the trabecular meshwork of rhesus monkey. Invest Ophthalmol 14:507, 1975.
18. Hogan MJ, Alvarado JA, and Weddel J: Histology of the Human Eye: An Atlas and Textbook. Chapter Four. Philadelphia, WB Saunders Co. 1971, p. 141.
19. Ogston AG, Preston BN, and Wells JD: On the transport of compact particles through solutions of long chain polymers. Proc Royal Soc A333:297, 1973.
20. Curry FE and Michel CC: A fiber matrix model of capillary permeability. Microvasc Res 20:96, 1980.
21. Jackson GW and James DF: The hydrodynamic resistance of hyaluronic acid and its contribution to tissue permeability. Biorheology 19:317, 1982.
22. Preston BN, Davies M, and Ogston AG: The composition and physicochemical properties of hyaluronic acids prepared from ox synovial fluid and from a case of mesothelomia. Biochem J 96:449, 1965.
23. Fessler JH: Mode of action of testicular hyaluronidase. Biochem J 76:132, 1960.
24. Fessler JH and Ogston AG: Studies on the sedimentation, diffusion and viscosity of some sarcosine polymers in aqueous solution. Trans Farad Soc 47:667, 1951.
25. Ethier CR: Hydrodynamics of Flow Through Gels with Applications to the Eye. SM Thesis, Department of Mechanical Eng., M.I.T., 1983.
26. Ogston AG and Sherman TF: Effects of hyaluronic acid upon diffusion of solutes and flow of solvent. J Physiol 156:67, 1961.
27. Johnstone MA and Grant WM: Pressure dependent changes in structures of the aqueous outflow system of human and monkey eyes. Am J Ophthalmol 75:365, 1973.
28. Morrison JC and Van Buskirk EM: The canine eye: pectinate ligaments and aqueous outflow resistance. Invest Ophthalmol Vis Sci 23:726, 1982.
29. Fatt I and Hedbys BO: Flow conductivity of human corneal stroma. Exp Eye Res 10:237, 1970.
30. Comper WD and Laurent TC: Physiological function of connective tissue polysaccharides. Physiol Rev 58:255, 1978.
31. Hascall VC and Hascall GK: Proteoglycans. *In* Cell Biology of Extracellular Matrix. Hay ED, editor. New York, Plenum Press, 1982, pp. 46–48.
32. Grant WM: Experimental aqueous perfusion in enucleated human eyes. Arch Ophthalmol 69:783, 1963.